Scripta Materialia 177 (2020) 74–78

Contents lists available at ScienceDirect

Scripta Materialia

journal homepage: www.elsevier.com/locate/scriptamat

Negative Poisson's ratio in Heusler-type Cu–Al–Mn shape memory alloy

Sheng Xu, Ryota Tsukuda, Mi Zhao, Xiao Xu, Toshihiro Omori, Kyosuke Yoshimi, Ryosuke Kainuma*

Department of Materials Science, Graduate School of Engineering, *Tohoku University*, 6-6-02 Aoba-yama, *Sendai 980-8579, Japan*

ARTICLE INFO

Article history:
Received 2 August 2019
Revised 9 October 2019
Accepted 9 October 2019

Keywords:
Negative Poisson's ratio
Shape memory alloy
Single crystal

ABSTRACT

A negative Poisson's ratio refers to the phenomenon of a material expanding along the transverse direction upon uniaxial tension. Here, we show a negative Poisson's ratio observed directly by experiments in a single-crystal Heusler-type Cu–16.9Al–11.6Mn (at%) shape memory alloy, in addition to the alloy's superelasticity. When stretched along the vicinity of the [110] direction, the alloy expands along the $[1\bar{1}0]$ direction, showing a significant negative Poisson's ratio of −0.51, while shrinking along the [001] direction with a large positive Poisson's ratio of 1.36. These experimental results agree well with the values calculated from the elastic constants and elastic anisotropy.

Poisson's ratio, which characterizes the transverse deformation response to a uniaxial stress, is a fundamental mechanical property of solid materials. Poisson's ratio is defined as the negative ratio of the transverse strain to the longitudinal strain in uniaxial tension or compression. Normally, this value is positive because most materials shrink along the transverse direction (TD) when they are stretched in the loading direction (LD), or expand along the TD upon uniaxial compression. However, a negative Poisson's ratio (NPR), that is, a counterintuitive expansion in the TD by uniaxial tension, is theoretically permissible. In isotropic linear elasticity, Poisson's ratio lies within the bounds of −1–0.5 [1]. For anisotropic solids, the allowed range is even broader [2].

Materials with NPR are called "auxetics" [3]. They have many potential technological applications, such as strain amplifiers, soundproofing components, and mechanical diodes (an auxetic material that just fits inside a tube can be inserted further but can be pulled out only with difficulty) [4,5]. The NPR was first reported in foams with open reentrant structures by Lakes [6], after which many materials engineered with similar structures showing NPR were reported [7]. The NPR has also been found in dense bulk crystalline solids, such as α-cristobalite [8,9] and cubic metals [10]. Baughman et al. correlated the work function with the NPR and proposed that the NPR is attainable for 69% of the cubic elemental metals [10]. The NPR in these cubic metals is believed to be intrinsic because it results from the internal atomic/electronic structures [10,11].

Cu_2MnAl is a typical Heusler intermetallic compound with an $L2_1$ ordered crystal structure, and is predicted to show a NPR of −0.34 along the $[1\bar{1}0]$ direction when stressed along the [110] direction [10]. By designing the off-stoichiometric compositions close to Cu_2MnAl, Heusler-type Cu-Al-Mn shape memory alloys with a high ductility were developed by our group in the 1990s [12]. The Cu-Al-Mn shape memory alloys crystallize in an $L2_1$ structured parent phase, and show excellent superelasticity due to the stress-induced martensitic transformation, as well as good cold workability [13]. Moreover, they can be prepared easily in large single crystals via abnormal grain growth by a recently developed cyclic heat treatment method [14,15]. In this study, we report, by direct experimental observations, an intrinsic NPR in a single-crystal bulk Heusler-type Cu-Al-Mn shape memory alloy. Thus, this alloy shows not only superelasticity but also auxetic elastic behavior.

A Cu-Al-Mn ingot bar with a diameter of around 40 mm was prepared by induction melting in an argon atmosphere. The chemical composition was determined to be Cu-16.9Al-11.6Mn (at%) using wavelength dispersive x-ray spectroscopy (WDS). After an intermediate annealing at 520 °C for 30 min, the ingot was cold drawn to 11 mm in diameter with an area reduction ratio of 92.4%. Single-crystal bars of around 300 mm long were then prepared using cyclic heat treatments via abnormal grain growth, with the details on cyclic heat treatments shown in Fig. 1(a). The large single crystal was oriented to near [110] along the long direction, which was confirmed by electron backscattered diffraction (EBSD). The single crystal was then aged at 200 °C for 15 min. Disc specimens were subjected to differential scanning calorimetry (DSC) measurement with a heating/cooling rate of 10 °C/min to

* Corresponding author.
E-mail address: kainuma@material.tohoku.ac.jp (R. Kainuma).

https://doi.org/10.1016/j.scriptamat.2019.10.015
1359-6462/

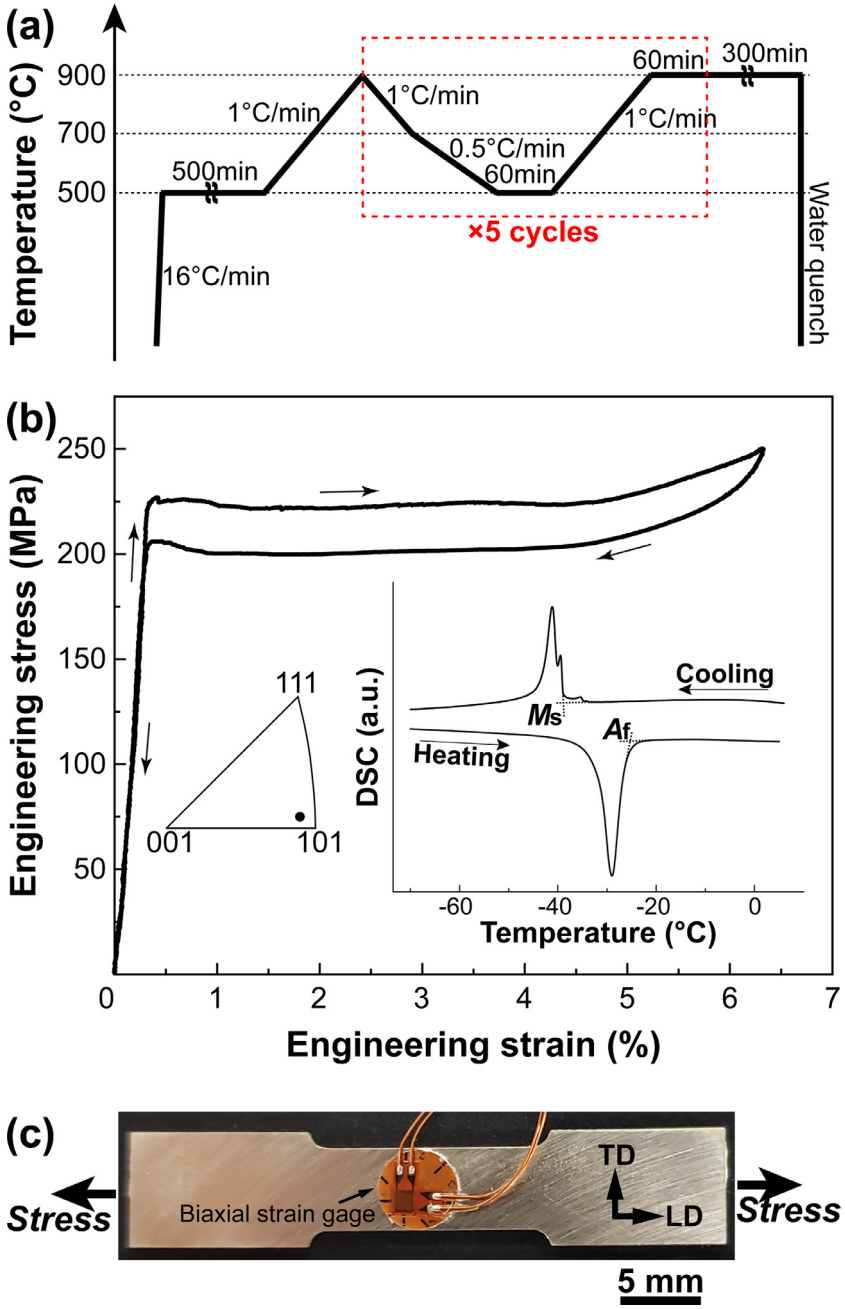

Fig. 1. (a) Cyclic heat treatments for the preparation of the large Cu–Al–Mn single crystal; (b) superelastic stress–strain curve of the present alloy at room temperature, the inset shows the DSC curves characterizing the martensitic transformation temperatures and (c) a single-crystal specimen prepared for measuring the Poisson's ratio, where the strains along the loading direction (LD) and the transverse direction (TD) can be measured simultaneously.

determine the martensitic transformation temperatures. The martensitic transformation starting (M_s) and reverse phase transformation finishing (A_f) temperatures were determined to be −39.0 °C and −25.6 °C, respectively, as shown in the inset of Fig. 1(b). The superelastic response was examined by a loading–unloading tensile test at room temperature with a strain rate of 1.0×10^{-4} s^{-1} using a dog-bone shaped specimen. The gage dimension of the specimen was about 13 mm × 5 mm × 0.8 mm, and the strain was measured by a noncontact video extensometer. The corresponding stress–strain curve is shown in Fig. 1(b). As can be seen, a phase transformation strain of more than 5% can be obtained once the critical stress of around 230 MPa is reached upon loading.

Single-crystal sheet specimens with an [110] orientation were prepared for tensile tests to directly determine the Poisson's ratio. The specimens were cut from the large single-crystal bar so as to have several typical orientations, such as [001], [$1\bar{1}2$], [$1\bar{1}1$] and [$1\bar{1}0$], in the TDs. The actual orientation slightly deviated from the designed one and was further determined by the EBSD technique. Tensile tests were conducted in loading–unloading mode at room temperature with a strain rate of 1×10^{-4} s^{-1}. Tensile specimens were prepared in a dog-bone shape with a gage dimension of about 13 mm × 5 mm × 0.8 mm. The maximum applied stress was set at 120 MPa, which is far below the critical stress for inducing martensitic transformation, to ensure an elastic deformation of the parent phase. The strains along the LD and TD were

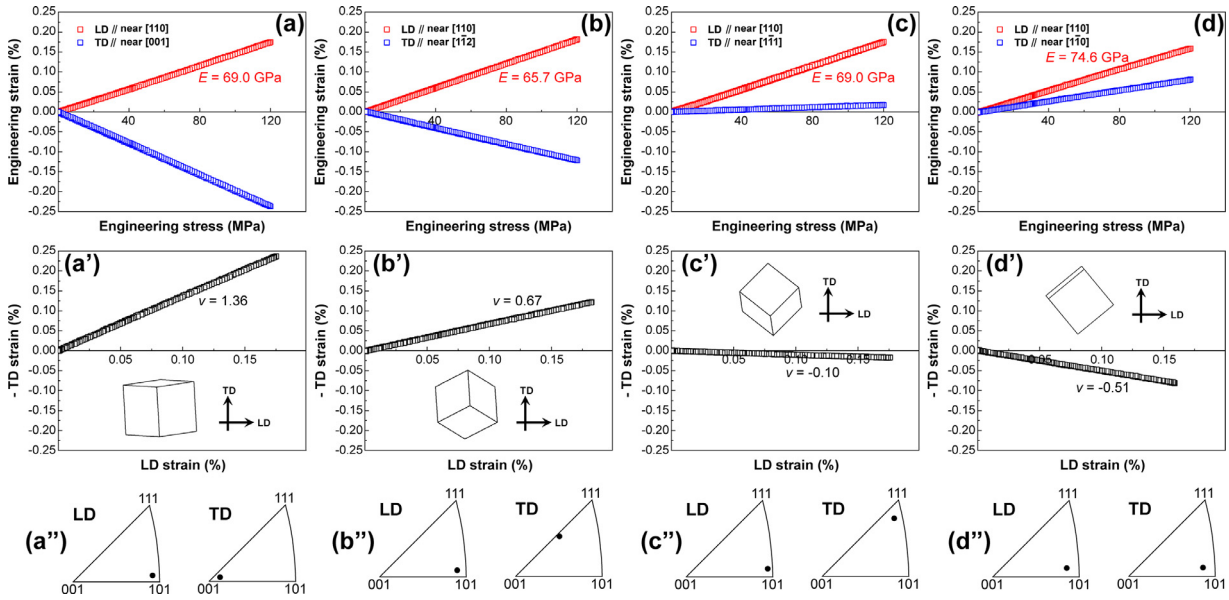

Fig. 2. (a)–(d) Stress–strain curves upon loading and unloading with the transverse direction (TD) aligned with different crystal orientations, the loading direction (LD) is fixed to near the [110] direction; (a')–(d') corresponding curves of minus strain along the TD vs strain along the LD; (a")–(d") inverse pole figures illustrating the crystal orientations along the LD and TD.

simultaneously measured using a biaxial strain gauge (KFG-1-120-D16-16, Kyowa) attached to the surface of the specimens, as shown in Fig. 1(c). The loading–unloading cycle was conducted at least three times for each specimen and excellent reproducibility was confirmed.

The elastic constants of the alloy were determined using the electromagnetic acoustic resonance (EMAR) method. A $5 \times 5 \times 5$ mm^3 single-crystal specimen was cut out by using electrical discharge machining (EDM). It had mutually perpendicular surfaces orientated in the [100], [010] and [001] directions, as confirmed by EBSD. EMAR measurement was performed on a commercial instrument (CCII-HT, Nihon Techno-Plus Co. Ltd.) at room temperature over a vibration frequency range of 200–1300 kHz in a magnetic field of 5 kOe. More details can be found in reference [16].

Fig. 2 depicts the experimental results of the stress–strain curves during tensile loading–unloading of the present single-crystal alloy, from which Poisson's ratios are directly measured. In Fig. 2(a)–(d), the stress–strain curves with the TDs aligned to near the [001], [1$\bar{1}$2], [1$\bar{1}$1] and [1$\bar{1}$0] directions are shown, respectively. The linear curves upon loading and unloading overlap, suggesting that these measurements were conducted within the range of elastic deformation of the parent phase. The averaged Young's modulus along the LD is 69.6 GPa. Correspondingly, the opposite strains along the TD are plotted against the strains along the LD in Fig. 2(a')–(d'), and the Poisson's ratios are deduced by the slope after linear fitting of data points. The inverse pole figures indicating the crystal orientations along the LD and TD are also shown in Fig. 2(a")–(d"). As can be identified, Poisson's ratio is strongly transverse orientation dependent when stretching along near the [110] direction. When the TD is along near the [001] direction, Poisson's ratio can be as large as 1.36, exceeding the upper boundary of isotropic elasticity. When the TD is along near the [1$\bar{1}$2] direction, Poisson's ratio remains positive with a large value of 0.67. However, both the LD and TD strains increase with the tensile stress when the TD is aligned to the [1$\bar{1}$0] direction, indicating a negative value of Poisson's ratio of −0.51. It is also worth noting that a near-zero Poisson's ratio of −0.10 appears when the TD is near the [1$\bar{1}$1] direction.

In anisotropic solids with a cubic crystal structure, the Poisson's ratio between the LD and TD can be explicitly expressed in terms of elastic constants by [11,17]

$$\nu(\boldsymbol{n}, \boldsymbol{m}) = \frac{(C_{11}+2C_{12})(C_{11}-C_{12}-2C_{44})D(\boldsymbol{n}, \boldsymbol{m}) + 2C_{12}C_{44}}{2(C_{11}+2C_{12})(C_{11}-C_{12})C_{44}} E(\boldsymbol{n}), \tag{1}$$

where

$$D(\boldsymbol{n}, \boldsymbol{m}) = n_1^2 m_1^2 + n_2^2 m_2^2 + n_3^2 m_3^2. \tag{2}$$

Here, $\boldsymbol{n}$ and $\boldsymbol{m}$ are orthogonal unit vectors corresponding to certain orientations in a cubic crystal, being parallel to the LD and TD, respectively. $E(\boldsymbol{n})$ is the Young's modulus along the $\boldsymbol{n}$, which is expressed as

$$\frac{1}{E(\boldsymbol{n})} = \frac{1}{3(C_{11}+2C_{12})} - \frac{1-3P(\boldsymbol{n})}{3(C_{11}-C_{12})} + \frac{1-P(\boldsymbol{n})}{2C_{44}}, \tag{3}$$

where

$$P(\boldsymbol{n}) = n_1^4 + n_2^4 + n_3^4. \tag{4}$$

In cubic crystals, the elastic anisotropy A, also known as the Zener ratio, is defined as $A = 2C_{44}/(C_{11}-C_{12})$. $A > 1$ is then featured in an elastically anisotropic cubic crystal, which means that $(C_{11}-C_{12}-2C_{44}) < 0$. Consequently, as seen from Eq. (1), the term $(C_{11}+2C_{12})(C_{11}-C_{12}-2C_{44})D(\boldsymbol{n},\boldsymbol{m})$ is the only term with a negative value, hence the Poisson's ratio could be negative when the absolute value of this term is large enough. In addition, the function $D(\boldsymbol{n},\boldsymbol{m})$ in Eq. (1) indicates the directional dependence of the Poisson's ratio. When the LD is fixed to the [100] or [111] direction, the value of $D(\boldsymbol{n},\boldsymbol{m})$ is constant, and therefore the Poisson's ratio is independent of the transverse orientation. However, when the LD is fixed to the [110] direction, the value of $D(\boldsymbol{n},\boldsymbol{m})$ ranges from 0 to 0.5, and the Poisson's ratio is consequently dependent on the transverse orientation.

Table 1 lists the elastic constants obtained by the EMAR method at room temperature for the present alloy. The condition $(C_{11}-C_{12}) > 0$ must be fulfilled to ensure elastic stability. The shear modulus C', which is the resistance to tetragonal deformation, was deduced by $C'=(C_{11}-C_{12})/2$ and is also listed in Table 1. The value of C' is

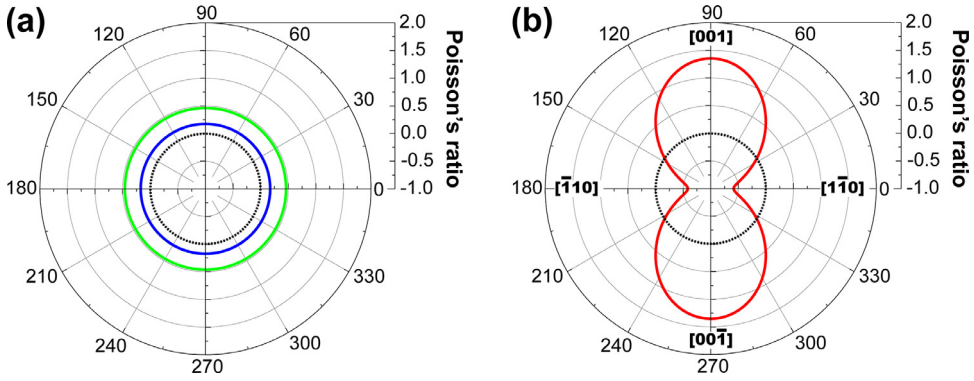

Fig. 3. (a) Dependence of Poisson's ratio on the transverse direction (TD) when the loading directions (LDs) are fixed to the [100] direction (green line) and the [111] direction (blue line), respectively and (b) Poisson's ratio varies by the TD when the LD is parallel to the [110] direction. The dashed line indicates the zero value of Poisson's ratio. (For interpretation of the references to color in this figure legend, the reader is referred to the web version of this article.)

Table 1
Experimentally determined room-temperature elastic constants of the parent phase of present Cu–Al–Mn alloy.

C_{11} (GPa)	C_{12} (GPa)	C_{44} (GPa)	C' (GPa)	A
129.2	110.3	97.6	9.5	10.3

low, which is a feature sometimes found in parent phases showing martensitic transformation, such as the case of Cu-Al-Ni shape memory alloys [18], indicating that the parent phase of the present Cu-Al-Mn alloy has dynamically low stability contributing to the transformation-induced superelasticity.

Using the elastic constants in Table 1 and Eq. (1), Poisson's ratios with several typical stretching directions are obtained. Fig. 3(a) depicts the calculated Poisson's ratios when the LDs are fixed to the [100] and [111] directions. It can be seen that, when stretched along the [100] or [111] directions, the crystal displays isotropic deformation along TDs, with the corresponding isotropic Poisson's ratios being 0.46 and 0.17, respectively. However, when stretched along the [110] direction, the crystal shows anisotropic Poisson's ratios with extremal values, as shown in Fig. 3(b). For example, when the TD parallels to the [001] direction, a maximum Poisson's ratio of 1.35 can be reached, while the minimum Poisson's ratio is −0.58 when the TD is along the [1$\bar{1}$0] direction. In addition, the Young's modulus of stressing along the [110] direction is calculated using Eq. (3) to be 81.1 GPa, which is slightly larger than the experimental values shown in Fig. 2(a)–(d). This discrepancy is probably caused by the deviated crystal orientation of the specimens and experimental errors.

It has also been suggested by Lethbridge et al. that the NPR can be predicted directly and simply by using the elastic anisotropy [19]. In their report, a normal central force and a tangential force are considered as the interaction between neighboring atoms to deduce the minimum Poisson's ratio, and that interaction is assumed to be a function of elastic anisotropy. Also, a simple atom-to-atom spring model was suggested to describe the maximum Poisson's ratio, where the spring constants were correlated with the elastic anisotropy. It is then claimed that the correlation between the value of elastic anisotropy and the magnitudes of minimum and maximum Poisson's ratios is independent of crystal symmetry and can be semi-empirically expressed as [19]

$$\nu_{\min} = (2 - A)/(A + 3), \tag{5}$$

$$\nu_{\max} = (4A - 1)/(2A + 7). \tag{6}$$

Here, $\nu_{\min}$ and $\nu_{\max}$ are the minimum and maximum Poisson's ratios, respectively. The parent phase of the present Cu-Al-Mn alloy is highly elastically anisotropic, as indicated by $A = 10.3$, listed in Table 1. The $\nu_{\min}$ and $\nu_{\max}$ for the present alloy are then estimated to be −0.62 and 1.46, respectively.

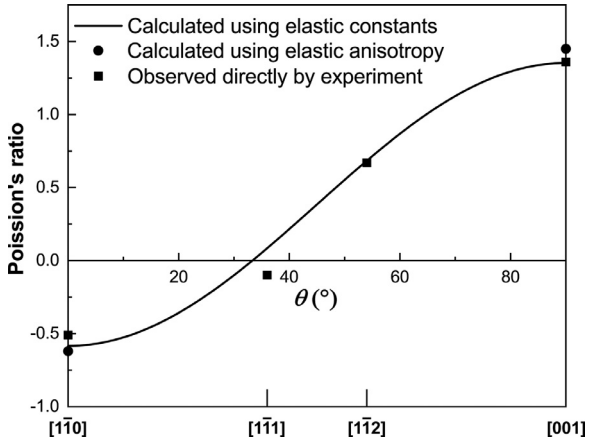

Fig. 4. Comparison of Poisson's ratios between experimental and calculated values when stretching along the [110] direction.

In Fig. 4, the solid line shows the Poisson's ratios calculated using Eq. (1) based on the experimentally determined elastic constants when the LD is fixed to the [110] direction, with the square dots showing the directly experimentally measured ones. The minimum and maximum Poisson's ratios calculated by Eqs. (5) and (6) using the elastic anisotropy are also included as round dots. The θ in the horizontal coordinate is the angle deviating from the [1$\bar{1}$0] direction in the TDs. Although the LD deviates slightly from the [110] direction of the experimental specimens, a good consistency can be seen among these results.

The NPR in the present Cu-Al-Mn shape memory alloy is an intrinsic property of the parent phase because neither phase transition nor macrostructure change was involved. Although NPR is a common feature in many cubic metals, as suggested by Baughman et al. [10], the present alloy has advantages over many others. First, the NPR during elastic deformation, combined with the superelastic deformation due to reversible stress-induced martensitic transformation, may provide new application possibilities for this alloy, such as in multi-switch or multi-step mechanical diodes. The Poisson's ratio during the martensitic transformation requires further investigation, though. Second, NPR generally requires that the specimens be in single crystals with a [110] orientation. Fortunately, large single crystals near the [110] orientation are easy to prepare by designing the initial recrystallization texture and subsequent abnormal grain growth for the present alloy [20,21]. This means that our Cu-Al-Mn alloy that shows NPR is promising for practical applications as an auxetic material.

In conclusion, we have experimentally studied the NPR behavior in a single-crystal Heusler-type Cu-16.9Al-11.5Mn (at%) shape memory alloy. The results show that when stretched along the vicinity of the [110] direction, the alloy shows Poisson's ratios ranging from positive to negative depending on the transverse orientation. Typically, the single crystal shows a NPR of −0.51 when the transverse orientation is near the $[1\bar{1}0]$ direction, a large positive Poisson's ratio of 1.36 when the transverse orientation is near the [001] direction, and a near-zero value of −0.10 when the transverse orientation is near the $[1\bar{1}1]$ direction. The experimental results are consistent with calculated values using experimentally determined elastic constants as well as the elastic anisotropy. Combined with the superelasticity and easy production of oriented single crystals, the Cu-Al-Mn shape memory alloy is a promising material for practical applications related to the NPR phenomenon.

Declaration of Competing Interest

None.

Acknowledgments

This work was financially supported by Grants-in-Aid for Scientific Research from the Japan Society for the Promotion of Science (JSPS, Grant Nos. 15H05766, 18J11979 and 19K22037). Dr. Sumio Kise at Furukawa Techno Material Co. Ltd. is acknowledged for his help in sample preparation.

References

[1] L.D. Landau, E.M. Lifshitz, Theory of Elasticity, 2nd ed., Pergamon, Oxford, 1995.
[2] M. Rovati, Scr. Mater. 48 (2003) 235–240.
[3] K.E. Evans, M.A. Nkansah, I.J. Hutchinson, S.C. Rogers, Nature 353 (1991) 124.
[4] K.E. Evans, Endeavour 15 (1991) 170–174.
[5] K.E. Evans, A. Alderson, Adv. Mater. 12 (2000) 617–628.
[6] R. Lakes, Science 235 (1987) 1038–1041.
[7] X. Yu, J. Zhou, H. Liang, Z. Jiang, L. Wu, Prog. Mater. Sci. 94 (2018) 114–173.
[8] A. Yeganeh-Haeri, D.J. Weidner, J.B. Parise, Science 257 (1992) 650–652.
[9] N.R. Keskar, J.R. Chelikowsky, Nature 358 (1992) 222–224.
[10] R.H. Baughman, J.M. Shacklette, A.A. Zakhidov, S. Stafström, Nature 392 (1998) 362–365.
[11] X.F. Wang, T.E. Jones, W. Li, Y.C. Zhou, Phy. Rev. B 85 (2012) 134108.
[12] R. Kainuma, S. Takahashi, K. Ishida, Metall. Mater. Trans. A 27 (1996) 2187–2195.
[13] Y. Sutou, T. Omori, J.J. Wang, R. Kainuma, K. Ishida, Mater. Sci. Eng. A 378 (2004) 278–282.
[14] T. Omori, T. Kusama, S. Kawata, I. Ohnuma, Y. Sutou, Y. Araki, K. Ishida, R. Kainuma, Science 341 (2013) 1500–1502.
[15] T. Kusama, T. Omori, T. Saito, S. Kise, T. Tanaka, Y. Araki, R. Kainuma, Nat. Commun. 8 (2017) 354.
[16] M. Zhao, K. Yoshimi, K. Maruyama, K. Yubuta, Acta Mater. 64 (2014) 382–390.
[17] T. Paszkiewicz, S. Wolski, Phys. Status Solidi B 244 (2007) 966–977.
[18] P. Sedlák, H. Seiner, M. Landa, V. Novák, P. Šittner, L. Mañosa, Acta Mater. 53 (2005) 3643–3661.
[19] Z.A. Lethbridge, R.I. Walton, A.S. Marmier, C.W. Smith, K.E. Evans, Acta Mater. 58 (2010) 6444–6451.
[20] Y. Sutou, T. Omori, K. Yamauchi, N. Ono, R. Kainuma, K. Ishida, Acta Mater. 53 (2005) 4121–4133.
[21] S. Xu, T. Kusama, X. Xu, H. Huang, T. Omori, J. Xie, R. Kainuma, Materialia 6 (2019) 10336.